Longitudinal Modulus and Hydraulic Permeability of Poly(methacrylic acid) Gels: Effects of Charge Density and Solvent Content

Thomas M. Quinn and Alan J. Grodzinsky*

Continuum Electromechanics Group, Laboratory for Electromagnetic and Electronic Systems, Department of Electrical Engineering and Computer Science, Massachusetts Institute of Technology, Cambridge, Massachusetts 02139

Received January 25, 1993; Revised Manuscript Received March 26, 1993

ABSTRACT: The equilibrium longitudinal modulus, hydraulic permeability, and fixed charge density of poly(methacrylic acid) gels were measured over a wide range of pH, ionic strength, and uniaxial strain (solvent content). Mechanical measurements were performed using a compression–stress relaxation procedure which was analyzed in the context of a poroelastic theory of gel swelling kinetics. The longitudinal modulus varied with ionization state and solvent content in a manner that suggests the importance of ionized charge density as a critical determinant of gel stiffness and swelling. The modulus decreased while the hydraulic permeability increased substantially with increasing gel solvent content. However, the kinetics of gel swelling were less sensitive to the initial gel solvent content than was the modulus or permeability individually, consistent with the predictions of poroelastic theory.

Introduction

Polyelectrolyte hydrogels can undergo large, rapid, and reversible changes in hydration (solvent:polymer volume ratio) as a result of swelling forces which arise due to ionization of the polymer matrix. These swelling forces may be modified dramatically by changes in environmental factors such as pH, ionic strength, and temperature.[1-6] In addition, externally applied electric fields may be used to alter pH and ionic strength distributions inside a gel,[7] providing a means for electrical control of gel deformations.[5,8,9] As a result, these materials have potential applications in areas as diverse as controlled drug delivery,[1,10,11] separation/purification processes,[4,12-16] "robot muscle",[17,18] and cell culture.[19] Many of these applications require rapid and accurate manipulation of gel hydration. A detailed understanding of the parameters that govern the dynamic swelling properties of polyelectrolyte hydrogels is therefore essential.

While many previous experiments have dealt with swelling equilibrium, less attention has been focused on the kinetics of swelling. In general, mechanical, chemical, or electrical (e.g., ionization) processes could be rate-limiting during the swelling of polyelectrolyte gels. For example, Tanaka and Fillmore[20] observed that for electrically neutral gel beads in a bath with no chemical potential gradients other than those of the solvent and polymer, mechanical processes alone governed swelling kinetics as described by the elastic moduli and hydraulic permeability of the gel. In contrast, changes in bath pH may lead to changes in ionization of a polyelectrolyte gel, which can induce swelling that is limited by slow chemical diffusion/reaction processes.[3,4,21] The dynamics of electrically stimulated swelling can be either mechanically or chemically rate-limited.[5,8,13]

In the present study we have investigated the longitudinal modulus and hydraulic permeability of poly(methacrylic acid) (PMAA) hydrogels over a wide range of pH (fixed charge density), ionic strength, and compressive strain (hydration). The objectives were (a) to quantify the contribution of electrostatic interactions to gel stiffness and permeability, and thereby to the mechanical parameters that govern the kinetics of gel swelling, and (b) to develop experimental and theoretical methodologies that enable measurement of modulus and permeability over a wide range of gel hydration.

Previously, the mechanical, chemical, and electrical parameters that govern the dynamics of gel swelling have been delineated within the context of specific theoretical models. Several models relevant to gel swelling have been developed. Biot's poroelastic theory of soil mechanics[22,23] describes the mechanical dynamics of deformation and fluid flow within a porous, elastic solid matrix permeated by a viscous, compressible fluid. Biot explicitly showed that mechanical deformations in such materials are described by governing laws that exhibit diffusion-like kinetics, with a diffusivity given by the product of an elastic stiffness parameter and a permeability parameter associated with viscous fluid flow relative to the solid matrix.[23] With the simplifying assumption of fluid incompressibility and the understanding that mechanical stiffness may be intimately related to both polymer and fluid properties in polyelectrolyte hydrogels, Biot's model has direct applications in models of gel swelling dynamics.[24]

Tanaka *et al.*[25,26] also used a poroelastic conceptualization in their development of a model for the kinetics of gel deformations. They used this model to interpret time correlations and intensity measurements of light scattered from density fluctuations (microscopic mechanical deformations) in poly(acrylamide) gels. Independent values of bulk modulus K, shear modulus μ, and permeability were obtained; the gel swelling kinetics were shown to be related to the product of the longitudinal modulus M (where $M = K + 4\mu/3$) and the hydraulic permeability. Tanaka and Fillmore[20] applied this model under conditions of negligible shear modulus to describe the macroscopic swelling kinetics of spherical 5% poly(acrylamide) gel beads in water. The "mechanical diffusivity" they observed was at least an order of magnitude smaller than the molecular diffusivity of water in such highly hydrated gels, confirming that the kinetics of swelling was rate-limited by mechanical transport processes and not chemical diffusion of the solvent in that experiment. Other investigators have extended this model to include shear modulus[27] and to describe dynamic swelling in cylindrical[28] and planar[29] geometries. Mow *et al.*[30] employed a mixture

* Author to whom correspondence should be addressed [telephone (617) 253-4969].

0024-9297/93/2226-4332$04.00/0

Table I. Reagents for the PMAA Hydrogel

amount	ingredient
10 mL	methacrylic acid (MAA; monomer)
50 μL	triethylene glycol dimethacrylate (TEGDMA; cross-linker)
2 mL	deionized water
3 mL	ethylene glycol
0.3 mL	40% (w/v) ammonium persulfate solution (AP; initiator)
0.3 mL	15% (w/v) sodium metabisulfite solution (SMBS; initiator)

theory approach in their development of a mechanical model for articular cartilage; they used stress relaxation and creep in a planar geometry to measure both longitudinal modulus and hydraulic permeability. The above theories have identified the mechanical rate processes that govern the swelling of materials with no gradients in chemical species other than solvent or polymer. Grodzinsky *et al.* have included chemical and electrical coupling in their models of cartilage[31,32] and polyelectrolyte gel[5,21] dynamics and have developed techniques of electromechanical spectroscopy[32] for the measurement of parameters including longitudinal modulus and hydraulic permeability. Swelling in these experiments was induced by changes in bath pH, salt content, or applied electric fields; hence, chemical and electrical rate processes that affect swelling kinetics were included in the models.

Grimshaw *et al.*[5] extended this work in their description of electromechanical and electrochemical coupling in planar polyelectrolyte hydrogel dynamics. They calculated the hydraulic permeability of PMAA hydrogels from independent electroosmosis data and measured longitudinal modulus using equilibrium compressive stress vs strain data. With these parameter values assumed to be constant during swelling, predictions compared reasonably well with chemically induced swelling data and with electrically induced swelling data when electroosmosis was neglected. This latter limitation may have been due to inadequate mechanical characterization of the gels studied; it was hypothesized[5] that detailed knowledge of variations of mechanical parameters with gel swelling state, pH, and ionic strength could be essential to accurately describe the rapid, coupled dynamics of electrically induced swelling. In the present study, we have tried to quantify these parameters and to identify the most important factors that contribute to their values over a wide range of pH, ionic strength, and compressive strain. Measurements were made with a stress relaxation technique developed in the context of the Grimshaw *et al.* model.[5]

Experimental Section

Preparation of PMAA Gels. PMAA gel membranes were cast between glass plates as previously described.[14,16] Table I lists the reagents for the PMAA gels used in this study (designated the S.05/1 formulation by Grimshaw *et al.*[16]). All reagents except initiators were mixed and degassed under vacuum for 10 min. Initiators were then added, and the mixture was pipetted between clean, dry glass plates separated by a 500-μm Teflon spacer. The plates were clamped together and placed in a 60 °C water bath for 4 h for gel polymerization. Four membranes 500 μm thick and roughly 30 cm^2 in surface area were cast at one time from a single reagent mixture. After casting, gel membranes were washed overnight in deionized water to remove reagents not incorporated into the gel polymer. Cylindrical disk samples 25 mm in diameter were then cut from each membrane using a circular cork borer and were placed in an unbuffered 50 mM KCl solution at pH ~11 for 2 days. Samples were then equilibrated for several days in 500-mL baths containing a fixed concentration of KCl (in the range 50 mM–1.0 M) at fixed pH (5 mM pH buffer was used in all cases). Baths were replaced with fresh solutions after the first day.

Table II. pH Values Studied in Stress Relaxation Experiment and pH Buffers Used

pH	buffer[a]	pH	buffer[a]
3.0	citric acid; $pK_1 = 3.06$	5.7	malonic acid; $pK_2 = 5.70$
4.7	citric acid; $pK_2 = 4.74$	6.8	imidazole; $pK = 7.00$
5.3	citric acid; $pK_3 = 5.40$		

[a] Buffers were used at a concentration of 5 mM.

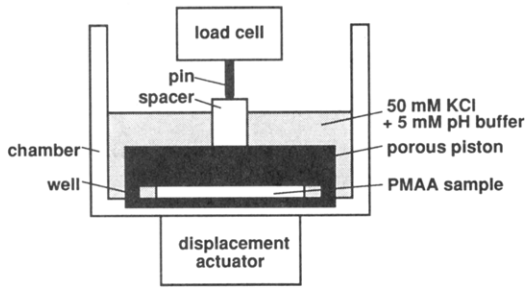

Figure 1. Schematic of the compression–stress relaxation apparatus.

Two studies were performed. In the first, samples from a single gel reagent mixture were equilibrated at fixed ionic strength (50 mM KCl) over a range of pH. Buffers used and pH values were listed in Table II. In the second study, samples from another gel reagent mixture were all equilibrated at pH ~6.8 over a range of bath ionic strength from 50 mM to 1 M KCl. In both studies, the free-swelling equilibrium water content (hydration) and fixed charge density (titration), the equilibrium longitudinal modulus, and the hydraulic permeability were measured as functions of bath pH and KCl concentration.

Hydration and Titration Measurements. Gel hydration (H) is defined as the volume ratio of gel solvent to polymer

$$H \equiv \frac{V_s}{V_p} = \frac{m_s}{m_p}\frac{\rho_p}{\rho_s} \tag{1}$$

where V_s and V_p are the volumes occupied by the solvent and polymer, respectively, and m and ρ denote mass and mass density, respectively. Specimen hydration was assessed from wet weight and dry weight measurements, as described previously[14] (see Appendix A for details). pH titration of gel specimens was performed using standard methods (see Appendix B for details).

Compression–Stress Relaxation Experiments. Transient compression–stress relaxation experiments were performed on PMAA gel samples having equilibrium hydrations spanning almost the entire range of hydration attainable for this gel formulation (ref 15 and below). The experiment utilized an ultrasensitive servo-controlled materials tester (Dynastat mechanical spectrometer, Dynastatics Instruments Corp., Latham, NY), which consisted of a displacement actuator and a load cell (Figure 1), with associated transducers and control electronics. The displacement actuator was used to control sample thickness with an accuracy of 1 μm, while the load cell measured the force required to maintain fixed thickness. The load cell could detect changes in stress as small as 25 Pa.

Equilibrated gel disk samples were trimmed to 21 mm diameter disks with a cork borer and centered in the bottom of a cylindrical polysulfone well 25.4 mm diameter by 4 mm deep (Figure 1). The disk was submerged in its equilibration solution in a polysulfone chamber mounted on the Dynastat displacement actuator. The solution circulated continuously between the chamber and a ~500-mL reservoir via a peristaltic pump. Reservoir temperature and pH were monitored to ensure stability. The sample communicated with the solution through a rigid, porous (27-μm pore size) stainless steel filter, 25.4 mm diameter by 3.2 mm thick (SSI Technologies Inc., Janesville, WI). The filter was then used as a porous piston to compress the gel in the thickness direction. Since the sample diameter was smaller than that of the well, compression was radially unconfined. However, the large diameter-to-thickness ratio of the sample disks (~20:1) and the high radial friction at the gel/piston interface (Figure 2a) ensured that swelling deformations were essentially uniaxial. (Thus, the radial strain at the disk periphery was assumed to be

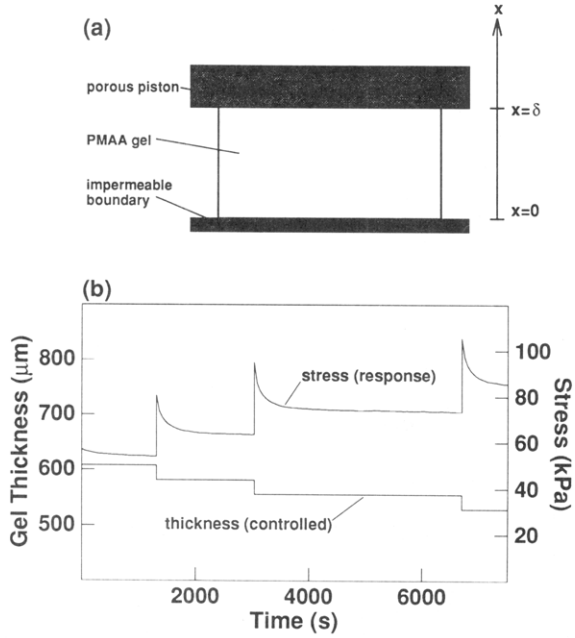

Figure 2. (a) Schematic of a cylindrical gel disk in uniaxial compression. (b) Example of a continuous recording of applied compression (gel thickness) and the resultant stress (calculated as the measured load normalized to the initial cross-sectional area).

negligible, consistent with the boundary condition required for measurement of the longitudinal modulus $M = K + 4\mu/3$ in uniaxial compression.) This was confirmed by comparison with confined compression measurements (data not shown). Loads on the porous filter were transmitted to the Dynastat load cell through a spacer and pin (Figure 1). The combined weight of the piston and spacer was 15 g, corresponding to less than 0.4 kPa preload on the gel disk.

With strain defined relative to the initial free-swelling (unstressed) equilibrium thickness at each pH, gel samples were compressed in increments of ~3% strain (using ramp compression times ~5 s) up to ~40% strain. Each increment in compressive strain caused the measured stress to increase sharply from the existing equilibrium (Figure 2b). Following each increment, sample thickness was held constant (for ~30 min) until the stress relaxed to a new equilibrium. The transient stress relaxation and final equilibrium stress data were recorded (e.g., Figure 2b) along with the imposed thickness. Thus, an equilibrium stress–strain curve was obtained for each specimen from experiments such as in Figure 2b, and the associated longitudinal modulus was calculated directly from the curve as a function of hydration (strain). The hydraulic permeability of each specimen was computed from the transient relaxation data using the following theoretical model for stress relaxation.

Theory: Stress Relaxation

When a gel is compressed, gradients in interstitial fluid pressure occur which produce fluid flow relative to the polymer network. The subsequent stress relaxation process involves redistribution of fluid and network elements within the gel until a new equilibrium state is achieved. We have used a limiting form of the model of Grimshaw *et al.*[5] to relate the measured stress relaxation time constant to the equilibrium longitudinal modulus of the gel network, M, and the hydraulic permeability, k, of the gel.

After 10–15 successive ~3% compressions of each gel disk (~40% total strain), a significant change in the ionization state of the carboxyl groups could occur due to the increased density of charge groups. However, for each individual ~3% compression, the change in carboxyl group ionization was assumed to be negligible. Therefore, the following theoretical development assumes that the gels were in electrochemical equilibrium during mechanical relaxation. It can also be shown[33] that electrokinetic coupling is negligible in our stress relaxation experiment. Therefore, only governing equations for mechanical dynamics are needed for an accurate theoretical description. For consistency with Grimshaw *et al.*, the appropriate limiting equations were taken from their one-dimensional, planar model for the coupled chemical, electrical, and mechanical dynamics of polyelectrolyte hydrogels.[5]

Darcy's law relates area-averaged fluid velocity U to gradients of fluid pressure P

$$U = -k(H,\bar{c}_i)\frac{\partial P}{\partial x} \tag{2}$$

where the hydraulic permeability k may in general be a function of hydration (H) and local ionic concentrations within the gel ($\bar{c}_i$). In the frame of the polymer, fluid continuity requires

$$\frac{\partial H}{\partial t} = -\frac{\partial U}{\partial \psi} \tag{3}$$

where ψ is a Lagrangian coordinate "attached" to the swellable polymer matrix ($d\psi = (1 + H)dx$). Polymer swelling stress σ is related to gel compressive strain ϵ by the longitudinal modulus M

$$\sigma = M(H,\bar{c}_i)\epsilon \tag{4}$$

where ϵ is defined in terms of hydration

$$\epsilon \equiv \frac{H_{eq}(\bar{c}_i) - H}{1 + H_{eq}(\bar{c}_i)} \tag{5}$$

H_{eq} represents the free-swelling equilibrium hydration at given conditions of $\bar{c}_i$. M may in general be a function of H and $\bar{c}_i$. In the absence of inertial effects, conservation of momentum requires a balance between fluid pressure P and polymer swelling stress σ throughout the gel:

$$(\partial/\partial x)(P + \sigma) = 0 \tag{6}$$

Equations 2–6 govern the behavior of the variables U, H, P, σ, and ϵ [all functions of space (x) and time (t)] subject to the local values of the parameters k, M, and H_{eq} (which are also functions of space and time since they depend on local values of H and $\bar{c}_i$). Grimshaw *et al.*[5] employed a more complete description including continuity equations for the $\bar{c}_i$; however, the above equations are sufficient to provide an accurate description of stress relaxation when transport of $\bar{c}_i$ is not rate-limiting, which we assume here.

Combining eqs 2 and 6 yields

$$U = k(H,\bar{c}_i)\frac{\partial \sigma}{\partial x} = k(H,\bar{c}_i)\left(\frac{\partial \sigma}{\partial H}\frac{\partial H}{\partial x} + \sum_i \frac{\partial \sigma}{\partial \bar{c}_i}\frac{\partial \bar{c}_i}{\partial x}\right) \tag{7}$$

where $\partial\sigma/\partial x$ has been expanded by treating σ as a function of H and $\bar{c}_i$, as indicated by eqs 4 and 5. Since H_{eq} is a function of $\bar{c}_i$ only, we may write

$$\sum_i \frac{\partial \sigma}{\partial \bar{c}_i}\frac{\partial \bar{c}_i}{\partial x} = \left(\sum_i \frac{\partial \sigma}{\partial \bar{c}_i}\frac{\partial \bar{c}_i}{\partial H_{eq}}\right)\frac{\partial H_{eq}}{\partial x} = 0 \tag{8}$$

where the second equality results because $\partial H_{eq}/\partial x$ is zero, since the local ion concentrations within the gel are assumed to be in electrochemical equilibrium with the external bath on the time scale of the mechanical stress relaxation experiment. Therefore, every point in the gel was "instantaneously" in equilibrium with the external bath, and all points had the same H_{eq}.

Using eqs 4 and 5, eq 7 may therefore be written

$$U = -\frac{1}{1+H_{eq}} M_\epsilon k \frac{\partial H}{\partial x} \tag{9}$$

where

$$M_\epsilon \equiv \frac{\partial \sigma}{\partial \epsilon} = M + \frac{\partial M}{\partial \epsilon}\epsilon \tag{10}$$

M_ϵ thus represents the local slope of the equilibrium stress vs strain curve, which was found to be nonlinear for large enough deformations.

At stress equilibrium for any imposed sample thickness, H was constant throughout the gel. Rapid gel compression required fluid loss through the porous piston, causing fluid loss in the upper region of the gel (Figure 2a). Subsequent stress relaxation involved fluid and polymer redistribution until uniform hydration was re-established. With the final equilibrium value of hydration following each stress relaxation represented by H_∞, hydration may be expressed

$$H(x,t) = H_\infty + \Delta H(x,t) \tag{11}$$

where $\Delta H(x,t)$ is a transient which must be zero at large times for all x. With consideration restricted to times large enough that $\Delta H(x,t)$ may be treated as a perturbation to H_∞, M_ϵ and k may be treated as constants corresponding to their values at H_∞. Incorporating eqs 9 and 11 into eq 3 yields a diffusion equation for $\Delta H(x,t)$.

$$\frac{\partial(\Delta H)}{\partial t} = \left(\frac{1+H_\infty}{1+H_{eq}}\right)(M_\epsilon k)\frac{\partial^2(\Delta H)}{\partial x^2} \tag{12}$$

This result is analogous to the diffusion-like poroelastic swelling kinetics described by Biot[23] for soils and by Tanaka and Fillmore[20] for poly(acrylamide) gels.

The condition of fixed thickness with one impermeable interface during stress relaxation requires zero fluid velocity at both gel surfaces (Figure 2a). Therefore, eqs 2, 4, 5, and 6 lead to the boundary conditions

$$\left.\frac{\partial(\Delta H)}{\partial x}\right|_{x=0} = \left.\frac{\partial(\Delta H)}{\partial x}\right|_{x=\delta} = 0 \tag{13}$$

Solution of eq 12 subject to eq 13 by separation of variables yields

$$\Delta H(x,t) = \sum_{n=1}^{\infty} A_n e^{-t/\tau_n} \cos\left(\frac{n\pi x}{\delta}\right) \tag{14}$$

where

$$\tau_n = \frac{1}{n^2}\frac{\delta\delta_{eq}}{\pi^2 M_\epsilon k} = \frac{1}{n^2}\tau_1 \tag{15}$$

Here, δ and δ_{eq} are the compressed and free-swelling sample thicknesses, respectively. It can be seen from eqs 4 and 5 that the measured stress varies directly as $\Delta H(\delta,t)$; hence eq 14 describes the kinetics of each stress relaxation at large times. Equation 15 shows that at times $t > \tau_1$, the terms of eq 14 with $n > 1$ do not contribute significantly to the kinetics; therefore, stress relaxation at $t > \tau_1$ can be described by the single-exponential time constant τ_1.

For each sample, the measured equilibrium stress/strain curve gave the "chord" modulus (i.e., the equilibrium longitudinal modulus) M and the "tangent" modulus M_ϵ as functions of strain. τ_1 was also measured for each stress relaxation, so that eq 15 could then be used to calculate k vs strain.

Results and Discussion

Hydration and Titration Measurements. To interpret the dependence of gel mechanical parameters on gel hydration and charge density, we first summarize the free-swelling equilibrium hydration and titration behavior of the gel (Figures 3 and 4). With increasing pH at 50 mM KCl, the gels were increasingly ionized (Figure 3). Equilibrium hydration concomitantly increased with pH (Figure 3) to such an extent that equilibrium fixed charge density (moles of polymer charge per liter of interstitial fluid) was relatively constant above pH ~4. For free-swelling gels equilibrated at constant pH ~6.8, equilibrium hydration decreased monotonically with increasing bath ionic strength (KCl concentration) up to 1 M (Figure 4). Also shown for comparison in Figure 4 is the calculated electrical Debye length, to be discussed below.

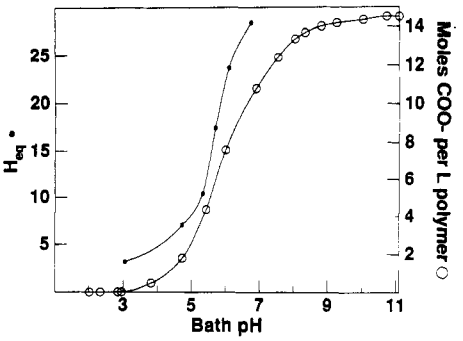

Figure 3. Free-swelling equilibrium hydration (H_{eq}) and polymer fixed charge vs pH for the PMAA gels in 50 mM KCl.

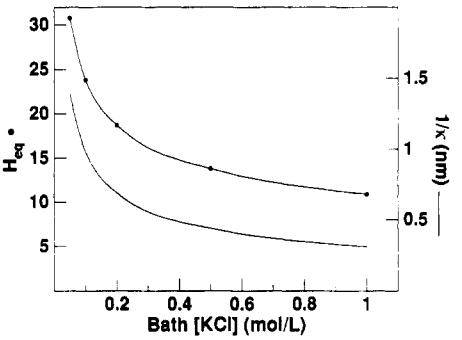

Figure 4. Free-swelling equilibrium hydration (H_{eq}) and theoretical Debye length ($1/\kappa$) vs bath [KCl] for PMAA gels at pH ~6.8. $1/\kappa$ was calculated from eq 16 by assuming $\epsilon = \epsilon_{water}$ and T = 300 K.

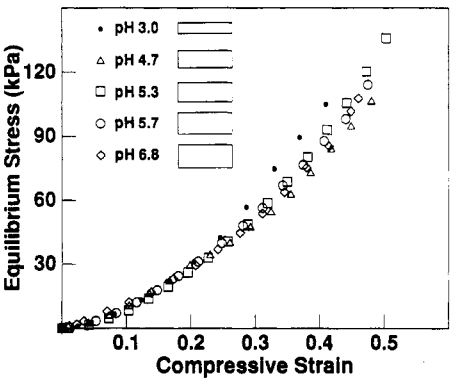

Figure 5. Equilibrium stress (σ) vs compressive strain (ϵ) of PMAA gels in 50 mM KCl at several values of pH ranging from 3.0 to 6.8. The relative free-swelling equilibrium thickness (δ_{eq}) at each pH is shown schematically.

Equilibrium Stress–Strain and Longitudinal Modulus: pH Dependence. Equilibrium stress vs compressive strain data for gels equilibrated in 50 mM KCl over a range of pH from ~3 to 7 are shown in Figure 5. In general, the longitudinal modulus M for these samples increased with compression, consistent with similar data obtained for biologically derived polyelectrolyte gels of comparable hydration and fixed charge

density.[34] The chord modulus M increased (almost linearly) from ~50 to ~250 kPa as strain increased up to ~40%, and the tangent modulus M_ϵ increased from ~50 to ~500 kPa. With strain defined relative to the free-swelling equilibrium hydration at each pH (as in eq 5), samples at the same strain had similar fixed charge densities (assessed from Figure 3). The similarity between the curves of Figure 5 indicates that the longitudinal modulus was determined by the fixed charge density as governed by the pH-dependent ionization and equilibrium hydration of the gel. Therefore, the charge density appears to be an important determinant of the longitudinal modulus and the overall equilibrium compressive stress/strain behavior of these gels, over a wide range of hydration.

For ionized polyelectrolyte hydrogels in compression, electrostatic effects governed by the density of fixed charge and the concentration of mobile counterions are expected to contribute much of the equilibrium stiffness[5,31,35] and swelling pressure.[10,36] Electrostatic interactions between fixed charges are mediated by mobile counterions; the characteristic length over which these interactions occur is known as the Debye length:[37]

$$\frac{1}{\kappa} = \left(\frac{\epsilon RT}{2z^2F^2c_{i0}}\right)^{1/2} \tag{16}$$

The Debye length ($1/\kappa$) varies inversely with both mobile ion valence (z) and the square root of bath ionic strength (c_{i0}). The electrostatic repulsion force per unit area (Π^{rep}) between flat plates having fixed charge per unit area σ_d, separated by a distance w, and immersed in an electrolyte-containing fluid with Debye length $1/\kappa$ and dielectric permittivity ϵ has been calculated[38] from the Poisson–Boltzmann equation and is given by

$$\Pi^{rep} = \frac{\sigma_d^2}{2\epsilon}\left[\frac{1}{\sinh(\kappa w/2)}\right]^2 \tag{17}$$

(Equation 17 applies when the electrical potential at the midpoint between the plates is small compared to the thermal voltage RT/F.[38]) This expression is not directly applicable to the molecules of the gel network of this study, for which a cylindrical rod geometry might be more appropriate. However, eq 17 contains the salient features of counterion-mediated electrostatic repulsion and is useful for further interpretation of the results of Figure 5. For this purpose, σ_d and w of eq 17 may be compared with the amount of fixed charge and the hydration (H), respectively. Thus, as the charge (σ_d) increased with increasing pH (Figure 3) at constant KCl concentration (constant κ), the hydration (w) also increased such that Π^{rep} remained approximately constant. Therefore, it seems reasonable that the data of Figure 5 were insensitive to pH changes.

Equilibrium Stress–Strain and Longitudinal Modulus: KCl Dependence. Equilibrium stress vs compressive strain data for gels equilibrated at pH ~6.8 over a range of KCl concentration from 0.05 to 1.0 M are shown in Figure 6. These data suggest that at pH ~6.8, where these gels were highly ionized (Figure 3), the longitudinal modulus was again influenced by the charge-dependent equilibrium hydration of the gel, in this case regulated by bath ionic strength. With increased ionic strength, the Debye length ($1/\kappa$) is reduced; this reduces the length scale of electrostatic interaction between charged gel molecules and counterions in the gel fluid phase and results in reduced equilibrium hydration, as seen in Figure 4. At equilibrium, the ratio of hydration to Debye length was similar for all samples (Figure 4); with strain

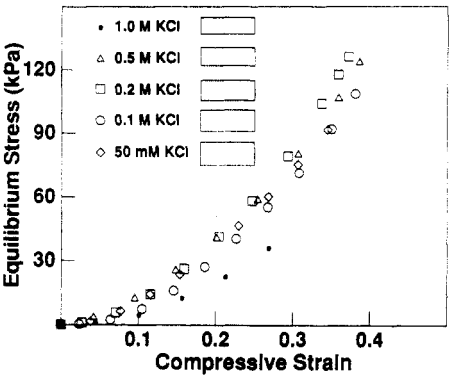

Figure 6. Equilibrium stress (σ) vs compressive strain (ϵ) of PMAA gels at pH ~6.8 in several bath KCl concentrations ranging from 0.05 to 1.0 M. The relative free-swelling equilibrium thickness (δ_{eq}) at each KCl concentration is shown schematically.

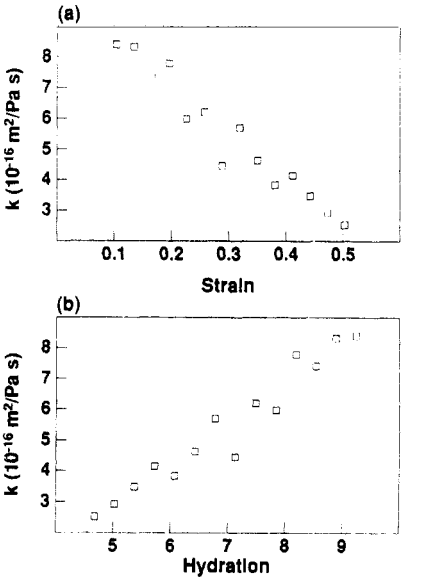

Figure 7. Hydraulic permeability k of PMAA gel in 50 mM KCl at pH 5.3 from stress relaxation experiment. Data are plotted (a) vs compressive strain ϵ and (b) vs hydration H.

defined relative to the free-swelling equilibrium hydration at each ionic strength, samples at the same strain would also have similar hydration:Debye length ratios. By analogy with eq 17, as $1/\kappa$ decreased, w decreased such that Π^{rep} remained constant; σ_d was constant in these samples. Therefore, it seems reasonable that the data of Figure 6 were insensitive to changes in ionic strength.

Hydraulic Permeability: pH Dependence. The hydraulic permeability of a PMAA disk equilibrated at pH 5.3 in 50 mM KCl is shown vs compressive strain in Figure 7a. The data points are the permeabilities computed from the stress relaxation curves produced by consecutive ~3% compressions applied to the gel. Equation 5 has been used to replot the same data vs hydration in Figure 7b. The permeability increased with increasing hydration as has been observed in other polyelectrolyte gels.[39]

Figure 8 shows permeability data for a series of specimens equilibrated in 50 mM KCl over a range of pH. A specimen was initially equilibrated at each specified pH (initial hydration was higher for specimens at higher pH, consistent with the data of Figure 3). Sequential ~3% compression–stress relaxation tests gave values for permeability vs increasing strain (decreasing hydration) shown for each specimen in Figure 8. The general trend of increased permeability with increased hydration was

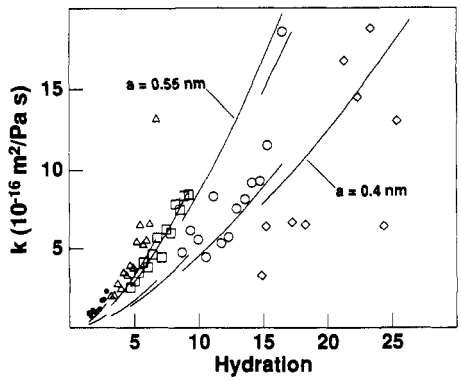

Figure 8. Hydraulic permeability k vs hydration for PMAA gels in 50 mM KCl: (●) pH 3.0; (△) pH 4.7; (□) pH 5.3; (○) pH 5.7; (◇) pH 6.8. The solid lines are the predictions of Happel's flow resistance model for two different assumed values of PMAA hydrodynamic radius (a).

consistent throughout. In addition, increased compressive strain appeared to decrease permeability at a given hydration. (For example, the pH 5.7 specimen compressed to hydration ~9 had lower permeability than the pH 5.3 specimen near its free-swelling hydration of ~9.) This may have been a result of compression-induced anisotropy of the gel polymer.

Happel's[40] unit cell model for the flow resistance of fiber matrices predicts that cylindrical rods aligned perpendicular to the flow direction of a viscous fluid present more flow resistance per unit volume than parallel-oriented rods. Modeling the gel polymer matrix of this study as a collection of cylindrical fibers aligned either parallel or perpendicular to the average fluid flow direction (i.e., the compression axis), the fraction of parallel-oriented rods $f_\parallel$ was treated as a linearly decreasing function of compressive strain ϵ:

$$f_\parallel = (1 - \epsilon)/3 \tag{18}$$

(Thus, at zero strain, a random three-dimensional matrix would have one-third of the fibers parallel and two-thirds perpendicular to flow in any direction, as is usually assumed.[40]) At a given hydration, the only adjustable parameter in Happel's model was the hydrodynamic radius a of the gel polymer fibers. Sedimentation experiments performed on other linear polymers[41] indicate that the hydrodynamic radius of the PMAA strands is expected to lie in the range 0.3–0.8 nm. Using effective hydraulic radii of 0.4 and 0.55 nm as lower and upper estimates in Happel's eqs 7 and 19,[40] Happel's model bounded the data and agreed with the order of magnitude and the overall trends (Figure 8). The model also suggested that uniaxially compressed gels might be expected to be less permeable to fluid flow than isotropically swollen gels at the same hydration, although this effect was smaller in the model than in the data.

Hydraulic Permeability: KCl Dependence. The hydraulic permeability of samples equilibrated at pH ~6.8 over a range of bath KCl concentrations increased with increasing hydration in a manner similar to that of Figure 8 (data not shown).

Conclusions

The longitudinal modulus of our PMMA gels varied with ionization state and hydration in a manner that suggests the importance of ionized charge density as a critical determinant of gel stiffness and swelling. The modulus decreased while the hydraulic permeability increased substantially with increasing gel hydration. Interestingly, since the time constant for stress relaxation (eq 15) (equivalent to the gel swelling time constant[20]) is determined by the product of M_ϵ and k, the kinetics of changes in gel swelling should be less sensitive to the initial gel hydration state than is M_ϵ or k individually. This hypothesis was confirmed by direct measurement of the gel swelling time constant over a wide range of gel hydration. The above results are particular to the gels prepared for this study; modifications in gel composition (e.g., cross-link density) could have significant effects on equilibrium hydration and other gel physical properties.[42,43]

The compression–stress relaxation techniques used in this study provided reasonably accurate measurements of longitudinal modulus and hydraulic permeability of PMAA hydrogels over a wide range of pH, ionic strength, and hydration. The theoretical basis of the measurements is in fact quite general and may be applied to any material that obeys the poroelastic governing laws; this should include a wide variety of polymer gels. Data obtained are useful for detailed modeling of swelling kinetics of gels and may also be valuable in the testing and refinement of microstructure-based models of longitudinal moduli[35,44,45] and hydraulic permeability.[40,46,47]

Acknowledgment. This research was supported by NSF Grant BCS-9111401 and NSF ERC Grant CDR-88-03014 to the Biotechnology Process Engineering Center at MIT. We thank Drs. Paul E. Grimshaw, Adi Shefer, and Eliot Frank for many helpful discussions and Ben Miller, Paul Mondani, and Sridhar Venkatesh for technical assistance.

Appendix A: Hydration Measurements

Assuming that $\rho_s = \rho_{water} = 1.0\ g/cm^3$ and using $\rho_p = 1.33\ g/cm^3$,[48] we have

$$H = 1.33\frac{m_s}{m_p} = 1.33\frac{m_{wet} - m_{dry}}{m_p}$$

where "wet" and "dry" sample masses have been introduced.

Samples were brought to equilibrium with baths of fixed pH and ionic strength. m_{wet} was measured for each sample by dabbing off surface water and weighing on a balance. Samples were then lyophilized for 1 day and weighed again for m_{dry}. m_p should have been the same for all samples prepared from a single reagent mixture. However, samples with significant fixed charge density (pH >5) contained a significant number of potassium ions which made $m_{dry} > m_p$. This was not a problem for samples equilibrated at pH ~3 in 50 mM KCl, for which $m_p = m_{dry}$ was an excellent approximation. Therefore, in both the pH and [KCl] studies, a few samples were equilibrated at pH ~3 in 50 mM KCl so that m_p could be determined for use in calculating the hydration (H) of all other samples.

Appendix B: pH Titration Measurements

Gel samples were preswollen in 50 mM KCl at pH ~11 (no buffer) and crushed into ~1-mm-sized chunks. These chunks were carefully rinsed into a beaker with a measured volume of 50 mM KCl at pH ~11 and maintained under a nitrogen atmosphere. HCl was added (using 100-μL aliquots of 1 M HCl) and pH was monitored with a pH meter and chart recorder to determine equilibrium after each addition. Titration to pH ~2 typically took 2 days; fluid volume and temperature did not vary significantly. For the gel formulation of this study, ~0.2% of the MAA carboxyl groups were attached to TEGDMA cross-linking molecules, assuming the ~50% cross-linking efficiency for these gels determined by Weiss *et al.*[42] The titration

data (Figure 3) for PMAA in 50 mM KCl resemble that of a Langmuir isotherm with an effective pK of ~6 and a maximum of ~14.5 mol charge/L of PMAA polymer.

References and Notes

(1) Peppas, N. A. *Recent Advances in Drug Delivery Systems*; Kim, S. W., Ed.; Plenum Press: New York, 1984.
(2) Osada, Y. *Adv. Polym. Sci.* **1987**, *82*, 1.
(3) Firestone, B. A.; Siegel, R. A. *Polym. Commun.* **1988**, *29*, 204.
(4) Gehrke, S. H.; Cussler, E. L. *Chem. Eng. Sci.* **1989**, *44*, 559.
(5) Grimshaw, P. E.; Nussbaum, J. H.; Grodzinsky, A. J.; Yarmush, M. L. *J. Chem. Phys.* **1990**, *93*, 4462.
(6) Okada, T.; Bae, Y. H.; Kim, S. W. *Pulsed and Self-Regulated Drug Delivery*; Kost, J., Ed.; CRC Press: Boca Raton, FL, 1990.
(7) Arndt, R. A.; Roper, L. D. *Simple Membrane Electrodiffusion Theory*; Physical Biological Sciences Misc.: Blacksburg, VA, 1972.
(8) Eisenberg, S. R.; Grodzinsky, A. J. *J. Membr. Sci.* **1984**, *19*, 173.
(9) Doi, M.; Matsumoto, M.; Hirose, Y. *Macromolecules* **1992**, *25*, 5504.
(10) Siegel, R. *Pulsed and Self-Regulated Drug Delivery*; Kost, J., Ed.; CRC Press: Boca Raton, FL, 1990.
(11) Grodzinsky, A. J.; Grimshaw, P. E. *Pulsed and Self-Regulated Drug Delivery*; Kost, J., Ed.; CRC Press: Boca Raton, FL, 1990.
(12) Henry, J. D.; Lawler, L. F.; Kuo, C. H. A. *AIChE J.* **1977**, *23*, 851.
(13) Grodzinsky, A. J.; Weiss, A. M. *Sep. Purif. Methods* **1985**, *14*, 1.
(14) Weiss, A. M.; Grodzinsky, A. J.; Yarmush, M. L. *AIChE Symp. Ser.* **1986**, *82* (250), 85.
(15) Grimshaw, P. E.; Grodzinsky, A. J.; Yarmush, M. L.; Yarmush, D. M. *Chem. Eng. Sci.* **1989**, *44*, 827.
(16) Grimshaw, P. E.; Grodzinsky, A. J.; Yarmush, M. L.; Yarmush, D. M. *Chem. Eng. Sci.* **1990**, *45*, 2917.
(17) de Rossi, D. E.; Chiarelli, P.; Buzzigoli, G.; Domenici, C.; Lazzeri, L. *Trans. Am. Soc. Artif. Intern. Organs* **1986**, *32*, 157.
(18) Shiga, T.; Hirose, Y.; Okada, A.; Kurauchi, T. *Polym. Prepr.* **1989**, *30*, 310.
(19) Gombotz, W. R.; Hoffman, A. S. *Hydrogels in Medicine and Pharmacy, I*; Peppas, N. A., Ed.; CRC Press: Boca Raton, FL, 1986.
(20) Tanaka, T.; Fillmore, D. J. *J. Chem. Phys.* **1979**, *70*, 1214.
(21) Nussbaum, J. H.; Grodzinsky, A. J. *J. Membr. Sci.* **1981**, *8*, 193.
(22) Biot, M. A. *J. Appl. Phys.* **1941**, *12*, 155.
(23) Biot, M. A. *J. Appl. Mech.* **1956**, *23*, 91.
(24) Johnson, D. L. *J. Chem. Phys.* **1982**, *77*, 1531.
(25) Tanaka, T.; Hocker, L. O.; Benedek, G. B. *J. Chem. Phys.* **1973**, *59*, 5151.
(26) Tanaka, T.; Ishiwata, S.; Ishimoto, C. *Phys. Rev. Lett.* **1977**, *38* (14), 771.
(27) Peters, A.; Candau, S. J. *Macromolecules* **1986**, *19*, 1952.
(28) Candau, S. J.; Peters, A. *Polym. Mater. Sci. Eng. Proc.* **1987**, *57*, 270.
(29) Chiarelli, P.; de Rossi, D. E. *Prog. Colloid Polym. Sci.* **1988**, *78*, 4.
(30) Mow, V. C.; Kuei, S. C.; Lai, M. W.; Armstrong, C. G. *J. Biomech. Eng.* **1980**, *102*, 73.
(31) Eisenberg, S. R.; Grodzinsky, A. J. *J. Biomech. Eng.* **1987**, *109*, 79.
(32) Frank, E. H.; Grodzinsky, A. J. *J. Biomechanics* **1987**, *20*, 629.
(33) Quinn, Thomas M. Master's thesis, Massachusetts Institute of Technology, Cambridge, MA, 1991.
(34) Hedbys, B. O.; Dohlman, C. H. *Exp. Eye Res.* **1963**, *2*, 122.
(35) Hasa, J.; Ilavsky, M.; Dusek, K. *J. Polym. Sci.* **1975**, *13*, 253.
(36) Rička, J.; Tanaka, T. *Macromolecules* **1984**, *17*, 2916.
(37) Debye, P.; Huckel, E. *Z. Phys.* **1923**, *24*, 185.
(38) Overbeek, J. Th. G. *Colloid Science, I*; Kruyt, H. R., Ed.; Elsevier Publishing: Amsterdam, 1952.
(39) Hedbys, B. O.; Mishima, S. *Exp. Eye Res.* **1962**, *1*, 262.
(40) Happel, J. *AIChE J.* **1959**, *5*, 174.
(41) Ogston, A. G.; Preston, B. N.; Wells, J. D. *Proc. R. Soc. London* **1973**, *333*, 297.
(42) Weiss, A. M.; Grodzinsky, A. J.; Yarmush, M. L. *J. Membr. Sci.* **1991**, *58*, 153.
(43) Flory, P. J. *Principles of Polymer Chemistry*; Cornell University Press: Ithaca, NY, 1953.
(44) Katchalsky, A.; Lifson, S. *J. Polym. Sci.* **1953**, *11*, 409.
(45) Lifson, S.; Katchalsky, A. *J. Polym. Sci.* **1954**, *13*, 43.
(46) Kuwabara, S. *J. Phys. Soc. Jpn.* **1959**, *14*, 527.
(47) Spielman, L.; Goren, S. L. *Environ. Sci. Technol.* **1968**, *2*, 279.
(48) Hasa, J.; Ilavsky, M.; Dusek, K. *J. Polym. Sci.* **1975**, *13*, 263.